 CMES, vol.43, no.3, pp.191-221, 2009

Transient Thermal Response of a Partially Insulated Crack in an Orthotropic Functionally Graded Strip under Convective Heat Supply

Yueting Zhou[1], **Xing Li**[2] **and Dehao Yu**[1]

Abstract: The transient response of an orthotropic functionally graded strip with a partially insulated crack under convective heat transfer supply is considered. It is modeled there exists thermal resistant in the heat conduction through the crack region. The mixed boundary value problems of the temperature field and displacement field are reduced to a system of singular integral equations in Laplace domain. The expressions with high order asymptotic terms for the singular integral kernel are considered to improve the accuracy and efficiency. The numerical results present the effect of the material nonhomogeneous parameters, the orthotropic parameters and dimensionless thermal resistant on the temperature distribution and the transient thermal stress intensity factors with different dimensionless time τ.

Keywords: orthotropic functionally graded materials (FGMs), convective heat transfer, thermal resistant, high order asymptotic term, transient thermal stress intensity factors.

1 Introduction

Functionally graded materials (FGMs) are multiple phase materials with spatially and continuously varying thermo-mechanical properties, which posses advantages such as maintaining the structural rigidity, reducing the thermal stress and resisting the severe thermal loading from the high temperature environment [Nino, Hirai, and Watanabe (1987); Suresh and Mortensen (1998); Miyamoto, Kaysser, Rabin, Kawasaki, and Ford (1999); Noda (1999); Yang, Qin, Zhuang, and You (2008)]. Through optimizing both material and component structures, functional gradation applies new opportunities to achieve high performance and material efficiency [Walters, Paulino, and Dodds Jr (2004)].

[1] LSEC, ICMSEC, Academy of Mathematics and Systems Science, CAS, Beijing 100190, China
[2] School of Mathematics and Computer Science, Ningxia University, Yinchuan 750021, China

Considerable investigations [Sladek, Sladek, V. and Krivacek (2005); Han, Pan, Roy, and Yue (2006); Sladek, Sladek, V. and Zhang (2003, 2007) ; Liu, Long, and Li (2008); Wen, Aliabadi, and Liu (2008); Oyekoya, Mba, and El-Zafrany (2008)] have been made in understanding the behavior of isotropic FGMs subjected to mechanical loading conditions. In studying the problems of FGMs, the anisotropic characters [Kaysser and Ilschner (1995); Gu and Asaro (1997)] should be considered due to the nature of processing techniques. Assuming an exponentially spatial variation of material properties, Ozturk and Erdogan (1997, 1999) investigated mode I and mixed-mode static crack problems in an infinite non-homogeneous orthotropic medium with integral equation method. Kim and Paulino (2002) investigated the mixed-mode static fracture problem of non-homogeneous orthotropic materials using finite element method [Liu and Yu (2008); Yu and Huang (2008); Liu, Zheng, and Liu (2009); Minutolo, Ruocco, and Ciaramella (2009); Sethuraman and Rajesh (2009); Shin, Huang, and Shiah (2009)] and the modified crack closure method, and compared the numerical results (FEM) for stress intensity factors (SIFs) with the semi-analytical solutions obtained by Ozturk and Erdogan (1997, 1999). For an orthotropic graded strip with a crack perpendicular to the boundary, the dynamic Mode I problem of an embedded crack [Chen, Liu, and Zou (2002)], the static Mode I problem of an edge crack [Guo, Wu, Zeng, and Ma (2004)], and the anti-plane impact problem[Chen and Liu (2005)] have been analyzed, respectively. Interface crack problems in an orthotropic graded coating-substrate system were solved by analytical and computational approaches [Dag, Yildirim, and Erdogan (2004)]. Sladek, Sladek, V. and Zhang (2005) conducted crack analysis in two-dimensional anisotropic FGMs with meshless local Petrov-Galerkin (MLPG) method.

FGMs have been developed initially to work in a super-high-temperature environment [Ootao and Tanigawa (2006)], the investigations of thermal properties [Ching and Chen (2006); Sladek, Sladek, V. Solek, Wen, and Atluri (2008)] for FGMs become more important. Assuming exponentially spatial variations in both elastic and thermal properties, Noda and Jin (1993) and Jin and Noda (1994) obtained solutions of thermal stress intensity factors (TSIFs) of internal crack and edge crack for isotropic infinite inhomogeneous materials subjected to steady thermal loading. Transient thermal stress intensity factors were also obtained for isotropic infinite inhomogeneous materials subjected to transient thermal loading [Jin and Noda (1994); Noda and Jin (1994); Jin and Batra (1996)]. Jin and Paulino (2001) studied an edge crack of an isotropic functionally graded strip under transient thermal loading conditions. Walters, Paulino, and Dodds Jr (2004) used a general domain integral method to obtain J-values along crack fronts in three-dimensional configurations of isotropic functionally graded materials. Jin and Feng (2008) investigated

the thermal fracture behavior of a functionally graded coating with periodic edge cracks. Guo, Noda, and Wu (2008) developed a piecewise-exponential model (PE model) to investigate a functionally graded plate with arbitrary thermo-mechanical properties and a crack normal to the surfaces. Few researchers investigated the thermal fracture problems of orthotropic functionally graded materials under thermal loading due the complexity. Wang, Han, and Du (2000) investigated the fracture behavior of a laminated orthotropic strip subjected to unsteady thermal loads. Itou (2004) solved thermal stresses for a crack in an interfacial laminated orthotropic nonhomogeneous layer between two dissimilar elastic half planes. Assuming exponentially spatial variations in both elastic and thermal properties, Chen, Soh, Liu, and Liu (2004) conducted static thermal fracture analysis of an orthotropic functionally graded strip and Chen (2005) obtained thermal static stress intensity factors for an interface crack in a graded orthotropic coating-substrate structure using singular equation method. Dag (2006) used a new computational method based on the equivalent domain integral (EDI) to conduct mode I fracture analysis of orthotropic functionally graded materials subjected to static thermal stresses. Recently, transient thermal stress intensity factors of orthotropic functionally graded materials with a crack were obtained [Zhou, Li, and Qin (2007)]. Sladek, Sladek, V. Tan, and Atluri (2008) solved transient heat conduction problems in three-dimensional anisotropic FGMs with meshless local Petrov-Galerkin (MLPG) method. In all above-mentioned papers about thermal fracture problem, it was assumed under constant temperature distribution and the crack surfaces were insulated, which is physically less realistic.

In this paper, the transient response of an orthotropic functionally graded strip with a crack under convective heat transfer supply is investigated. It is assumed that the crack is partially insulated [El-Borgi, Erdogan, and Hatira (2003); El-Borgi, Erdogan, and Hidri (2004)], the temperature drop across the crack surfaces is the result of the thermal resistant due to the heat conduction through the crack region.

Laplace transform and Fourier transform are applied to reduce the mixed boundary value problems of the temperature field and displacement field to a system of singular integral equations [Yu (1993, 2002); Li (2008); Zhou, Li, and Yu (2008)] in Laplace domain. In the numerical computation process, the asymptotic expressions with high order terms for the singular integral kernels are considered. By using the numerical Laplace inversion method, the variations of the temperature distribution along the crack surfaces and extended line and transient thermal stress intensity factors with different time are presented. The influence of the material nonhomogeneous parameters, the orthotropic parameters and dimensionless thermal resistant on the temperature distribution and the transient thermal stress intensity factors is analyzed.

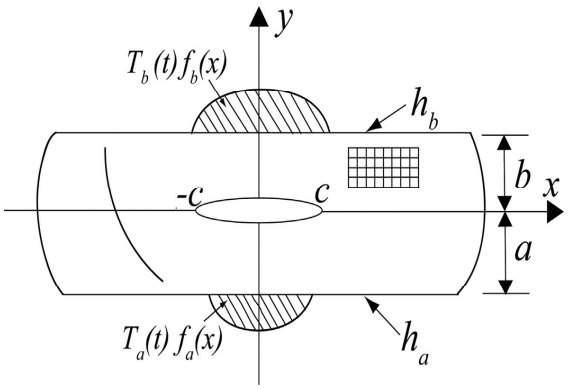

Figure 1: Geometry of the crack problem of orthotropic FGM strip with convective heat transfer supply.

2 Problem description and formulation

As shown in Figure 1, a through crack with its length being $2c$ exists in an orthotropic functionally graded strip. The strip is initially at the uniform temperature zero, and its surfaces $x=-a$ and $x=b$ are suddenly heated from the environment media with relative surface heat transfer coefficients h_a and . The environment temperatures are $T_a(t)f_a(x)$ and $T_b(t)f_b(x)$, respectively. We assume that $T_a(t)f_a(x)$ and $T_b(t)f_b(x)$ can be Fourier and Laplace transformed.

In this paper, plane stress state is considered. The thermal flux and stresses in dimensionless form can be expressed as follows

$$\begin{aligned}
&\overline{q}_x=-\overline{k}_x\frac{\partial\overline{T}}{\partial\overline{x}},\quad \overline{q}_y=-\overline{k}_y\frac{\partial\overline{T}}{\partial\overline{y}}\\
&\overline{\sigma}_{xx}=\overline{C}_{11}\frac{\partial\overline{u}}{\partial\overline{x}}+\overline{C}_{12}\frac{\partial\overline{v}}{\partial\overline{y}}-\overline{\theta}_1\overline{T},\quad \overline{\sigma}_{yy}=\overline{C}_{12}\frac{\partial\overline{u}}{\partial\overline{x}}+\overline{C}_{22}\frac{\partial\overline{v}}{\partial\overline{y}}-\overline{\theta}_2\overline{T}\\
&\overline{\sigma}_{xy}=\overline{C}_{66}\left(\frac{\partial\overline{u}}{\partial\overline{y}}+\frac{\partial\overline{v}}{\partial\overline{x}}\right)
\end{aligned}\tag{1}$$

with

$$\overline{\theta}_1=\overline{C}_{11}\overline{\alpha}_{xx}+\overline{C}_{12}\overline{\alpha}_{yy},\quad \overline{\theta}_2=\overline{C}_{12}\overline{\alpha}_{xx}+\overline{C}_{22}\overline{\alpha}_{yy},\quad \overline{C}_{66}=\overline{G}_{xy}\tag{2}$$

where $\overline{q}_j$ and $\overline{\sigma}_{ij}$ are thermal flux and stresses in dimensionless form, respectively; $\overline{k}_j$, $\overline{C}_{ij}$, $\overline{G}_{xy}$ and $\overline{\alpha}_{ii}$ are dimensionless form of the thermal conductivity coefficients, the elastic stiffness coefficients, the shear modulus and the linear thermal expansion coefficients, respectively.

The dimensionless form of the elastic stiffness coefficients, the linear thermal expansion coefficients and the thermal conductivity coefficients are modeled as follows

$$\begin{aligned}&(\overline{C}_{11},\overline{C}_{12},\overline{C}_{22},\overline{C}_{66}) = (\overline{C}^0_{11},\overline{C}^0_{12},\overline{C}^0_{22},\overline{C}^0_{66})\exp(\beta\overline{y})\\&(\overline{\alpha}_{xx},\overline{\alpha}_{yy}) = (\overline{\alpha}^0_{xx},\overline{\alpha}^0_{yy})\exp(\gamma\overline{y}),\quad (\overline{k}_x,\overline{k}_y) = (\overline{k}_{x1},\overline{k}_{y1})\exp(\delta\overline{y})\end{aligned} \tag{3}$$

where β, γ and δ are graded parameters to describe the nonhomogeneous material distribution. The elastic stiffness coefficients can be represented by the Young's modules and Poisson's ratios as

$$\overline{C}^0_{11} = \frac{\overline{E}^0_{xx}}{1-\nu_{yx}\nu_{xy}},\quad \overline{C}^0_{22} = \frac{\overline{E}^0_{yy}}{1-\nu_{yx}\nu_{xy}},\quad \overline{C}^0_{12} = \frac{\overline{E}^0_{yy}\nu_{xy}}{1-\nu_{yx}\nu_{xy}} \tag{4}$$

where Poisson's ratios ν_{ij} are assumed to be constant. Substituting Eq. (3) into Eq. (2), following can be obtained

$$\overline{\theta}_1 = \overline{\theta}^0_1\exp[(\beta+\gamma)\overline{y}],\quad \overline{\theta}_2 = \overline{\theta}^0_2\exp[(\beta+\gamma)\overline{y}] \tag{5}$$

where

$$\overline{\theta}^0_1 = \overline{C}^0_{11}\overline{\alpha}^0_{xx}+\overline{C}^0_{12}\overline{\alpha}^0_{yy},\quad \overline{\theta}^0_2 = \overline{C}^0_{12}\overline{\alpha}^0_{xx}+\overline{C}^0_{22}\overline{\alpha}^0_{yy} \tag{6}$$

In expressions (1)-(6), following dimensionless values are introduced

$$\begin{aligned}&\overline{T} = T/T_0,\quad (\overline{k}_x,\overline{k}_y,\overline{k}_{x1},\overline{k}_{y1}) = (k_x,k_y,k_{x1},k_{y1})/k_0,\quad (\overline{x},\overline{y}) = (x,y)/c\\&(\overline{q}_x,\overline{q}_y) = (q_x,q_y)c/(T_0k_0),\quad \overline{\sigma}_{ij} = \frac{\sigma_{ij}}{\alpha_0E_0T_0}(i,j=x,y),\quad (\overline{u},\overline{v}) = \frac{(u,v)}{\alpha_0T_0c}\\&(\overline{C}_{ij},\overline{G}_{xy},\overline{C}^0_{ij},\overline{G}^0_{xy}) = \frac{(C_{ij},G_{xy},C^0_{ij},G^0_{xy})}{E_0},\quad (i,j=1,2),\quad (\overline{E}^0_{xx},\overline{E}^0_{yy}) = \frac{(E^0_{xx},E^0_{yy})}{E_0}\\&(\overline{\alpha}_{ij},\overline{\alpha}^0_{ij}) = \frac{(\alpha_{ij},\alpha^0_{ij})}{\alpha_0},\quad (i,j=x,y)\end{aligned} \tag{7}$$

where T_0 is the reference temperature, k_0, α_0 and E_0 are the typical values of the thermal conductivity coefficient, the linear thermal expansion coefficient and the Young's module of elasticity, respectively.

Substituting Eqs. (1), (3) and (5) into the equilibrium equations, we can obtain following dimensionless governing equations for temperature and displacement field

$$\overline{k}_{10}\frac{\partial^2\overline{T}}{\partial\overline{x}^2}+\delta\frac{\partial\overline{T}}{\partial\overline{y}}+\frac{\partial^2\overline{T}}{\partial\overline{y}^2} = \frac{\partial\overline{T}}{\partial\tau} \tag{8}$$

$$\overline{C}_{11}^0 \frac{\partial^2 \overline{u}}{\partial \overline{x}^2} + \overline{C}_{66}^0 \frac{\partial^2 \overline{u}}{\partial \overline{y}^2} + (\overline{C}_{12}^0 + \overline{C}_{66}^0) \frac{\partial^2 \overline{v}}{\partial \overline{x} \partial \overline{y}} + \beta \overline{C}_{66}^0 (\frac{\partial \overline{u}}{\partial \overline{y}} + \frac{\partial \overline{v}}{\partial \overline{x}}) = \overline{\theta}_1^0 e^{\gamma \overline{y}} \frac{\partial \overline{T}}{\partial \overline{x}} \tag{9}$$

$$\overline{C}_{22}^0 \frac{\partial^2 \overline{v}}{\partial \overline{y}^2} + \overline{C}_{66}^0 \frac{\partial^2 \overline{v}}{\partial \overline{x}^2} + (\overline{C}_{12}^0 + \overline{C}_{66}^0) \frac{\partial^2 \overline{u}}{\partial \overline{x} \partial \overline{y}} + \beta (\overline{C}_{12}^0 \frac{\partial \overline{u}}{\partial \overline{x}} + \overline{C}_{22}^0 \frac{\partial \overline{v}}{\partial \overline{y}}) = \overline{\theta}_2^0 e^{\gamma \overline{y}} \left[(\beta + \gamma) \overline{T} + \frac{\partial \overline{T}}{\partial \overline{y}} \right] \tag{10}$$

where $\tau = D_2 \cdot t / c^2$ is dimensionless time, $D_2 = k_2 / c_v$ is the principal thermal diffusivity along principal axis y with ρ and c_v referring mass density and specific heat, respectively. is given as follows

$$\overline{k}_{10} = \overline{k}_{x1} / \overline{k}_{y1} \tag{11}$$

For the stated problem, the dimensionless thermal initial and thermal boundary conditions are

$$\overline{T} = 0, \quad \tau = 0 \tag{12}$$

$$\frac{\partial \overline{T}(\overline{x}, -\overline{a}, \tau)}{\partial \overline{y}} - H_a \cdot \overline{T}(\overline{x}, -\overline{a}, \tau) = -H_a \cdot \overline{T_a}(\tau) \cdot f_a(\overline{x}), \quad \tau > 0 \tag{13}$$

$$\frac{\partial \overline{T}(\overline{x}, \overline{b}, \tau)}{\partial \overline{y}} + H_b \cdot \overline{T}(\overline{x}, \overline{b}, \tau) = H_b \cdot \overline{T_b}(\tau) \cdot f_b(\overline{x}), \quad \tau > 0 \tag{14}$$

$$\frac{\partial \overline{T}(\overline{x}, 0^+, \tau)}{\partial \overline{y}} = -Bi \cdot \left(\overline{T}(\overline{x}, 0^+, \tau) - \overline{T}(\overline{x}, 0^-, \tau) \right), \quad |\overline{x}| \le 1 \tag{15}$$

$$\overline{T}(\overline{x}, 0^+, \tau) = \overline{T}(\overline{x}, 0^-, \tau), \quad |\overline{x}| > 1 \tag{16}$$

$$\partial \overline{T}(\overline{x}, 0^+, \tau) / \partial \overline{y} = \partial \overline{T}(\overline{x}, 0^-, \tau) / \partial \overline{y}, \quad |\overline{x}| < +\infty \tag{17}$$

and the mechanical boundary conditions are

$$\overline{\sigma}_{xy}(\overline{x}, -\overline{a}, \tau) = \overline{\sigma}_{yy}(\overline{x}, -\overline{a}, \tau) = 0, \quad |\overline{x}| < \infty \tag{18}$$

$$\overline{\sigma}_{xy}(\overline{x}, \overline{b}, \tau) = \overline{\sigma}_{yy}(\overline{x}, \overline{b}, \tau) = 0, \quad |\overline{x}| < \infty \tag{19}$$

$$\overline{\sigma}_{xy}(\overline{x}, 0, \tau) = \overline{\sigma}_{yy}(\overline{x}, 0, \tau) = 0, \quad |\overline{x}| \le 1 \tag{20}$$

$$\overline{\sigma}_{xy}(\overline{x}, 0^+, \tau) = \overline{\sigma}_{xy}(\overline{x}, 0^-, \tau), \overline{\sigma}_{yy}(\overline{x}, 0^+, \tau) = \overline{\sigma}_{yy}(\overline{x}, 0^-, \tau), \quad |\overline{x}| < \infty \tag{21}$$

$$\overline{u}(\overline{x}, 0^+, \tau) = \overline{u}(\overline{x}, 0^-, \tau), \quad \overline{v}(\overline{x}, 0^+, \tau) = \overline{v}(\overline{x}, 0^-, \tau), \quad |\overline{x}| > 1 \tag{22}$$

where

$$(\overline{T_a}, \overline{T_b}) = (T_a, T_b) / T_0, \quad (\overline{a}, \overline{b}) = (a, b) / c, \quad (H_a, H_b) = (h_a, h_b) c \tag{23}$$

Equation (15) indicates the temperature drop across the crack surfaces is the result of the thermal resistant contributed by the heat conduction through the crack region. In this equation, the quantity $Bi = c/k_{y1}/R_c$ is the dimensionless thermal resistant and R_c is the thermal resistant through the crack region. It is the ratio of the resistant $\frac{c}{k_{y1}}$ due to FGM thermal conduction at $\bar{y} = 0$ to crack region thermal resistant R_c.

Introduce following Laplace transform pair:

$$f^*(p) = \int_0^\infty f(\tau) e^{-p\tau} d\tau, \quad f(\tau) = \frac{1}{2\pi i} \int_{Br} f^*(p) e^{p\tau} dp \tag{24}$$

where Br represents the Bromwich path of integration.

Employing the Laplace transform to Eqs. (8)-(10), we can obtain

$$\bar{k}_{10} \frac{\partial^2 \overline{T}^*}{\partial \bar{x}^2} + \delta \frac{\partial \overline{T}^*}{\partial \bar{y}} + \frac{\partial^2 \overline{T}^*}{\partial \bar{y}^2} = p\overline{T}^* \tag{25}$$

$$\overline{C}^0_{11} \frac{\partial^2 \overline{u}^*}{\partial \bar{x}^2} + \overline{C}^0_{66} \frac{\partial^2 \overline{u}^*}{\partial \bar{y}^2} + (\overline{C}^0_{12} + \overline{C}^0_{66}) \frac{\partial^2 \overline{v}^*}{\partial \bar{x} \partial \bar{y}} + \beta \overline{C}^0_{66} \left(\frac{\partial \overline{u}^*}{\partial \bar{y}} + \frac{\partial \overline{v}^*}{\partial \bar{x}} \right) = \overline{\theta}^0_1 e^{\gamma \bar{y}} \frac{\partial \overline{T}^*}{\partial \bar{x}} \tag{26}$$

$$\overline{C}^0_{22} \frac{\partial^2 \overline{v}^*}{\partial \bar{y}^2} + \overline{C}^0_{66} \frac{\partial^2 \overline{v}^*}{\partial \bar{x}^2} + (\overline{C}^0_{12} + \overline{C}^0_{66}) \frac{\partial^2 \overline{u}^*}{\partial \bar{x} \partial \bar{y}} + \beta \left(\overline{C}^0_{12} \frac{\partial \overline{u}^*}{\partial \bar{x}} + \overline{C}^0_{22} \frac{\partial \overline{v}^*}{\partial \bar{y}} \right) = \overline{\theta}^0_2 e^{\gamma \bar{y}} \left[(\beta + \gamma) \overline{T}^* + \frac{\partial \overline{T}^*}{\partial \bar{y}} \right] \tag{27}$$

where $\overline{T}^*(\bar{x}, \bar{y}, p)$, $\overline{u}^*$ and $\overline{v}^*$ are the Laplace transforms of $\overline{T}(\bar{x}, \bar{y}, \tau)$, $\overline{u}$ and $\overline{v}$, respectively.

The thermal boundary conditions in the $p-$plane are

$$\frac{\partial \overline{T}^*(\bar{x}, -\bar{a}, p)}{\partial \bar{y}} - H_a \cdot \overline{T}^*(\bar{x}, -\bar{a}, p) = -H_a \cdot \overline{T_a}^*(p) \cdot f_a(\bar{x}) \tag{28}$$

$$\frac{\partial \overline{T}^*(\bar{x}, \bar{b}, p)}{\partial \bar{y}} + H_b \cdot \overline{T}^*(\bar{x}, \bar{b}, p) = H_b \cdot \overline{T_b}^*(p) \cdot f_b(\bar{x}) \tag{29}$$

$$\frac{\partial \overline{T}^*(\bar{x}, 0^+, p)}{\partial \bar{y}} = -Bi \cdot \left(\overline{T}^*(\bar{x}, 0^+, p) - \overline{T}^*(\bar{x}, 0^-, p) \right), \quad |\bar{x}| \le 1 \tag{30}$$

$$\overline{T}^*(\bar{x}, 0^+, p) = \overline{T}^*(\bar{x}, 0^-, p), \quad |\bar{x}| > 1 \tag{31}$$

$$\partial \overline{T}^*(\bar{x}, 0^+, p)/\partial \bar{y} = \partial \overline{T}^*(\bar{x}, 0^-, p)/\partial \bar{y}, \quad |\bar{x}| < +\infty \tag{32}$$

where $\overline{T_a}^*(p)$and $\overline{T_b}^*(p)$ are the Laplace transforms of $\overline{T_a}(\tau)$ and $\overline{T_b}(\tau)$, respectively.

The mechanical boundary conditions in the p-plane are

$$\overline{\sigma}^*_{xy}(\bar{x},-\bar{a},p)=\overline{\sigma}^*_{yy}(\bar{x},-\bar{a},p)=0, \quad |\bar{x}|<\infty \tag{33}$$

$$\overline{\sigma}^*_{xy}(\bar{x},\bar{b},p)=\overline{\sigma}^*_{yy}(\bar{x},\bar{b},p)=0, \quad |\bar{x}|<\infty \tag{34}$$

$$\overline{\sigma}^*_{xy}(\bar{x},0,p)=\overline{\sigma}^*_{yy}(\bar{x},0,p)=0, \quad |\bar{x}|\le 1 \tag{35}$$

$$\overline{\sigma}^*_{xy}(\bar{x},0^+,p)=\overline{\sigma}^*_{xy}(\bar{x},0^-,p),\overline{\sigma}^*_{yy}(\bar{x},0^+,p)=\overline{\sigma}^*_{yy}(\bar{x},0^-,p), \quad |\bar{x}|<\infty \tag{36}$$

$$\overline{u}^*(\bar{x},0^+,p)=\overline{u}^*(\bar{x},0^-,p), \quad \overline{v}^*(\bar{x},0^+,p)=\overline{v}^*(\bar{x},0^-,p), \quad |\bar{x}|>1 \tag{37}$$

where $\overline{\sigma}^*_{ij}$ are Laplace transforms of $\overline{\sigma}_{ij}$.

3 Temperature field

Employing Fourier transforms to Equation (25), we can obtain

$$\begin{aligned}
\overline{T}^*(\bar{x},\bar{y},p)&=\int_{-\infty}^{\infty}\sum_{j=1}^{2}A_j e^{n_j\bar{y}}e^{-i\bar{x}\omega}d\omega, \quad 0<\bar{y}\le\bar{b}\\
\overline{T}^*(\bar{x},\bar{y},p)&=\int_{-\infty}^{\infty}\sum_{j=1}^{2}B_j e^{n_j\bar{y}}e^{-i\bar{x}\omega}d\omega, \quad -\bar{a}\le\bar{y}\le 0
\end{aligned} \tag{38}$$

where $A_j(\omega)$ and $B_j(\omega)(j=1,2)$ are unknown functions and n_1,n_2 are the roots of the characteristic polynomials associated with the differential equation (25) and are given by

$$n^2+\delta\cdot n-(p+\bar{k}_{10}\omega^2)=0 \tag{39}$$

$$n_1=-\frac{\delta}{2}-\sqrt{\frac{\delta^2}{4}+p+\bar{k}_{10}\omega^2}, \quad n_2=-\frac{\delta}{2}+\sqrt{\frac{\delta^2}{4}+p+\bar{k}_{10}\omega^2} \tag{40}$$

Following density function is introduced

$$\varphi^*(\bar{x},p)=\frac{\partial\overline{T}^*(\bar{x},0^+,p)}{\partial\bar{x}}-\frac{\partial\overline{T}^*(\bar{x},0^-,p)}{\partial\bar{x}} \tag{41}$$

The unknown functions $A_j(\omega)$ and $B_j(\omega)$ $(j=1,2)$ in Eq. (38) can be expressed in term of $\varphi^*(\bar{x},p)$ with considering the boundary conditions (28), (29), (31) and

(32), and are given as follows

$$\begin{aligned}
A_1 &= \Omega_1^{(1)} \frac{i}{2\pi\omega} \int_{-1}^{1} \varphi^*(\bar{x},p) e^{i\omega\bar{x}} d\bar{x} + \Omega_1^{(2)} \overline{T_b}^* \widetilde{f}_b(\omega) + \Omega_1^{(3)} \overline{T_a}^* \widetilde{f}_a(\omega) \\
A_2 &= \Omega_2^{(1)} \frac{i}{2\pi\omega} \int_{-1}^{1} \varphi^*(\bar{x},p) e^{i\omega\bar{x}} d\bar{x} + \Omega_2^{(2)} \overline{T_b}^* \widetilde{f}_b(\omega) + \Omega_2^{(3)} \overline{T_a}^* \widetilde{f}_a(\omega) \\
B_1 &= \Omega_3^{(1)} \frac{i}{2\pi\omega} \int_{-1}^{1} \varphi^*(\bar{x},p) e^{i\omega\bar{x}} d\bar{x} + \Omega_3^{(2)} \overline{T_b}^* \widetilde{f}_b(\omega) + \Omega_3^{(3)} \overline{T_a}^* \widetilde{f}_a(\omega) \\
B_2 &= \Omega_4^{(1)} \frac{i}{2\pi\omega} \int_{-1}^{1} \varphi^*(\bar{x},p) e^{i\omega\bar{x}} d\bar{x} + \Omega_4^{(2)} \overline{T_b}^* \widetilde{f}_b(\omega) + \Omega_4^{(3)} \overline{T_a}^* \widetilde{f}_a(\omega)
\end{aligned} \tag{42}$$

where $\Omega_i^{(j)} (i = 1, \cdots, 4, j = 1,2,3)$ are given in Appendix A and $\widetilde{f}_a(\omega), \widetilde{f}_b(\omega)$ are the Fourier transforms of $f_a(\bar{x}), f_b(\bar{x})$, respectively.

Considering the remaining thermal boundary condition (30), we obtain following integral equation in which the unknown function is $\varphi^*(\bar{x},p)$

$$\begin{aligned}
&\lim_{\bar{y}\to 0^+} \int_{-1}^{+1} \int_{0}^{\infty} K(\omega,\bar{y},p) \sin[\omega(\eta-\bar{x})] \varphi^*(\eta,p) d\eta d\omega = \\
&-2\pi \int_{-\infty}^{\infty} \left[K_b \cdot \overline{T_b}^* \widetilde{f}_b(\omega) + K_a \cdot \overline{T_a}^* \widetilde{f}_a(\omega) \right] e^{-i\omega\bar{x}} d\omega
\end{aligned} \tag{43}$$

where the kernel $K(\omega,\bar{y},p)$ and known functions K_a, K_b are given in Appendix A.

Accounting for the singularity of the stated problem, we perform the asymptotic analysis of $K(\omega,\bar{y},p)$. As ω approaches infinity, following asymptotic expansion of $K(\omega,0,p)$ can be obtained

$$K^{(\infty)}(\omega,0,p) = a^{(0)} + \frac{a^{(1)}}{\omega} + \frac{a^{(2)}}{\omega^2} + \frac{a^{(4)}}{\omega^4} + \cdots + \frac{a^{12}}{\omega^{12}} + \frac{a^{(14)}}{\omega^{14}} + O(\frac{1}{\omega^{15}}) \tag{44}$$

where the superscript (∞)stands for the asymptotic expansion as $\omega \to \infty$, $a^{(j)} (j = 0,1,2,4,\cdots,12,14)$ are longthy expression of $Bi, \delta, \bar{k}_{10}$ and p, which are given in Appendix A.

Separating the singular parts of the kernel in Eq. (43), a singular integral equation can be obtained

$$\begin{aligned}
&\int_{-1}^{1} \left[\frac{\sqrt{\bar{k}_{10}}}{\eta-\bar{x}} + h(\bar{x},\eta,p) \right] \varphi^*(\eta,p) d\eta = \\
&\qquad -2\pi \int_{-\infty}^{\infty} \left[K_b \cdot \overline{T_b}^* \widetilde{f}_b(\omega) + K_a \cdot \overline{T_a}^* \widetilde{f}_a(\omega) \right] e^{-i\omega\bar{x}} d\omega
\end{aligned} \tag{45}$$

with kernel

$$h(\bar{x},\eta,p)=\int_0^L\left(K(\omega,0,p)-a^{(0)}-\frac{a^{(1)}}{\omega}\right)\sin[\omega(\eta-\bar{x})]d\omega+$$
$$\int_L^\infty\Big(K(\omega,0,p)-K^{(\infty)}(\omega,0,p)\Big)\sin[\omega(\eta-\bar{x})]d\omega$$
$$+\int_L^\infty\left(K^{(\infty)}(\omega,0,p)-a^{(0)}-\frac{a^{(1)}}{\omega}\right)\sin[\omega(\eta-\bar{x})]d\omega+\frac{\pi}{2}a^{(1)}sign(\eta-\bar{x}) \quad (46)$$

where $sign(\cdot)$ is signal function, L is an integration cut-off point, which is arbitrary positive real number and can be determined appropriately in numerical process. The first integral in the right hand side of Eq. (46) can be computed numerically using Gauss-Quadrature technique. The second integral in the right hand side of Eq. (46) tends to zero when L reaches sufficiently large [Dag (2001)]. The third integral in the right hand side of Eq. (46) can be evaluated in closed form; the formulae used to compute this type integral are given in Appendix B.

The single-value condition is

$$\int_{-1}^{1}\varphi^*(\eta,p)d\eta=0 \quad (47)$$

Based on the numerical method, $\varphi^*(s,p)$ can be expressed as

$$\varphi^*(\eta,p)=\frac{R(\eta,p)}{\sqrt{1-\eta^2}},\quad R(\eta,p)=\sum_{n=1}^{N}a_nT_n(\eta) \quad (48)$$

A system of linear algebraic equations can be obtained by using Gauss-Chebyshev formula

$$\sum_{l=1}^{N}\left[\frac{\sqrt{\bar{k}_{10}}}{s_l-r_m}+K(r_m,s_l,p)\right]\frac{R(s_l,p)}{N}=$$
$$-2\pi\int_{-\infty}^{\infty}\left[K_b\cdot\overline{T_b}^*\widetilde{f}_b(\omega)+K_a\cdot\overline{T_a}^*\widetilde{f}_a(\omega)\right]e^{-i\cdot\omega\cdot r_m}d\omega \quad (49)$$

$$\sum_{l=1}^{N}\frac{\pi\cdot R(s_l,p)}{N}=0 \quad (50)$$

where

$$s_l=\cos(\frac{2l-1}{2N}\pi)\quad(l=1,\cdots,N),\quad r_m=\cos(\frac{m}{N}\pi)\quad(m=1,\cdots,N-1) \quad (51)$$

The numerical solution of the temperature in the p-plane can be obtained from Eq. (38). The numerical solution of the temperature in the time domain can be obtained employing numerical inversion method of the Laplace transform proposed by Miller and Guy (1966).

4 Displacement field

Employing Fourier transforms to both sides of Eqs. (26) and (27), it can be shown that

$$\begin{aligned}
\overline{u}^* &= \int_{-\infty}^{\infty} \sum_{j=1}^{4} C_j e^{m_j \overline{y}} e^{-i\omega\overline{x}} d\omega + \int_{-\infty}^{\infty} \sum_{j=1}^{2} A_{1j} A_j e^{(\gamma+n_j)\overline{y}} e^{-i\omega\overline{x}} d\omega \\
\overline{v}^* &= \int_{-\infty}^{\infty} \sum_{j=1}^{4} C_j s_j e^{m_j \overline{y}} e^{-i\omega\overline{x}} d\omega + \int_{-\infty}^{\infty} \sum_{j=1}^{2} A_{2j} A_j e^{(\gamma+n_j)\overline{y}} e^{-i\omega\overline{x}} d\omega \quad 0 < \overline{y} \le \overline{b}
\end{aligned} \tag{52}$$

$$\begin{aligned}
\overline{u}^* &= \int_{-\infty}^{\infty} \sum_{j=1}^{4} C_{j+4} e^{m_j \overline{y}} e^{-i\omega\overline{x}} d\omega + \int_{-\infty}^{\infty} \sum_{j=1}^{2} A_{1j} B_j e^{(\gamma+n_j)\overline{y}} e^{-i\omega\overline{x}} d\omega \\
\overline{v}^* &= \int_{-\infty}^{\infty} \sum_{j=1}^{4} C_{j+4} s_j e^{m_j \overline{y}} e^{-i\omega\overline{x}} d\omega + \int_{-\infty}^{\infty} \sum_{j=1}^{2} A_{2j} B_j e^{(\gamma+n_j)\overline{y}} e^{-i\omega\overline{x}} d\omega \quad -\overline{a} \le \overline{y} \le 0
\end{aligned} \tag{53}$$

where $C_j (j = 1, \cdots, 8)$ are unknown functions determined from the boundary conditions (33), (34), (36) and (37) in the *time*-plane, and $m_j (j = 1, \cdots, 4)$ are the roots of the characteristic polynomial associated with the displacement equations Eqs. (26) and (27), which are given by

$$m^4 + 2\beta m^3 + (\beta^2 + \Delta_1) m^2 + \beta \Delta_1 m + \Delta_2 = 0 \tag{54}$$

with

$$\Delta_1 = \omega^2 \left(\frac{(\overline{C}_{12}^0)^2}{\overline{C}_{22}^0 \overline{C}_{66}^0} - \frac{\overline{C}_{11}^0}{\overline{C}_{66}^0} + 2\frac{\overline{C}_{12}^0}{\overline{C}_{22}^0} \right), \quad \Delta_2 = \omega^4 \frac{\overline{C}_{11}^0}{\overline{C}_{22}^0} + \omega^2 \beta^2 \frac{\overline{C}_{12}^0}{\overline{C}_{22}^0} \tag{55}$$

$s_j (j = 1, \cdots, 4)$ are given by

$$s_j = \frac{i\omega [m_j (\overline{C}_{12}^0 + \overline{C}_{66}^0) + \beta \overline{C}_{12}^0]}{m_j (m_j + \beta) \overline{C}_{22}^0 - \omega^2 \overline{C}_{66}^0} \tag{56}$$

and $A_{ij}(i,j=1,2)$ are given as

$$A_{1j}=\frac{i\omega\left\{(\gamma+n_j)(\gamma+n_j+\beta)(\overline{\theta}_2^0\overline{C}_{12}^0-\overline{\theta}_1^0\overline{C}_{22}^0)+\overline{C}_{66}^0[\omega^2\overline{\theta}_1^0+(\gamma+n_j+\beta)^2\overline{\theta}_2^0]\right\}}{\Lambda_j(\omega)}$$
$$A_{2j}=\frac{\omega^2\left\{(\gamma+n_j+\beta)(\overline{\theta}_1^0\overline{C}_{12}^0-\overline{\theta}_2^0\overline{C}_{11}^0)+(\gamma+n_j)\overline{C}_{66}^0[\omega^2\overline{\theta}_1^0+(\gamma+n_j+\beta)^2\overline{\theta}_2^0]\right\}}{\Lambda_j(\omega)} \tag{57}$$

in which

$$\Lambda_j(\omega)=$$
$$\overline{C}_{66}^0\left\{\omega^4\overline{C}_{11}^0+\omega^2[(\gamma+n_j)^2+(\gamma+n_j+\beta)^2]\overline{C}_{12}^0+(\gamma+n_j)^2(\gamma+n_j+\beta)^2\overline{C}_{22}^0\right\}$$
$$+\omega^2(\gamma+n_j)(\gamma+n_j+\beta)[(\overline{C}_{12}^0)^2-\overline{C}_{11}^0\overline{C}_{22}^0],(j=1,2) \tag{58}$$

Substituting Eqs. (38), (52) and (53) into Eq. (1), following dimensionless thermal stresses can be obtained

$$\overline{\sigma}_{yy}^*(\overline{x},\overline{y},\tau)=\int_{-\infty}^{\infty}\sum_{j=1}^{4}p_jC_je^{m_j\overline{y}}e^{-i\omega\overline{x}}e^{\beta\overline{y}}d\omega+\int_{-\infty}^{\infty}\sum_{j=1}^{2}q_jA_je^{(\gamma+n_j)\overline{y}}e^{-i\omega\overline{x}}e^{\beta\overline{y}}d\omega$$
$$\overline{\sigma}_{xy}^*(\overline{x},\overline{y},\tau)=\int_{-\infty}^{\infty}\sum_{j=1}^{4}r_jC_je^{m_j\overline{y}}e^{-i\omega\overline{x}}e^{\beta\overline{y}}d\omega+\int_{-\infty}^{\infty}\sum_{j=1}^{2}t_jA_je^{(\gamma+n_j)\overline{y}}e^{-i\omega\overline{x}}e^{\beta\overline{y}}d\omega,$$
$$0<\overline{y}\le\overline{b} \tag{59}$$

$$\overline{\sigma}_{yy}^*(\overline{x},\overline{y},\tau)=\int_{-\infty}^{\infty}\sum_{j=1}^{4}p_jC_{j+4}e^{m_j\overline{y}}e^{-i\omega\overline{x}}e^{\beta\overline{y}}d\omega+\int_{-\infty}^{\infty}\sum_{j=1}^{2}q_jB_je^{(\gamma+n_j)\overline{y}}e^{-i\omega\overline{x}}e^{\beta\overline{y}}d\omega$$
$$\overline{\sigma}_{xy}^*(\overline{x},\overline{y},\tau)=\int_{-\infty}^{\infty}\sum_{j=1}^{4}r_jC_{j+4}e^{m_j\overline{y}}e^{-i\omega\overline{x}}e^{\beta\overline{y}}d\omega+\int_{-\infty}^{\infty}\sum_{j=1}^{2}t_jB_je^{(\gamma+n_j)\overline{y}}e^{-i\omega\overline{x}}e^{\beta\overline{y}}d\omega,$$
$$-\overline{a}\le\overline{y}\le 0 \tag{60}$$

where

$$\begin{aligned}
p_j &= -i\omega\overline{C}_{12}^0 + s_j m_j \overline{C}_{22}^0, \quad (j=1,\cdots,4)\\
q_j &= -i\omega A_{1j}\overline{C}_{12}^0 + A_{2j}(\gamma+n_j)\overline{C}_{22}^0 - \overline{\theta}_2^0 \quad (j=1,2)\\
r_j &= (m_j - i\omega s_j)\overline{C}_{66}^0, \quad (j=1,\cdots,4)\\
t_j &= [A_{1j}(\gamma+n_j) - i\omega A_{2j}]\overline{C}_{66}^0, \quad (j=1,2)
\end{aligned} \tag{61}$$

We now introduce two density functions

$$\begin{aligned}
\varphi_1^*(\bar{x},p) &= \frac{\partial}{\partial\bar{x}}[\overline{u}^*(\bar{x},0^+,p) - \overline{u}^*(\bar{x},0^-,p)]\\
\varphi_2^*(\bar{x},p) &= \frac{\partial}{\partial\bar{x}}[\overline{v}^*(\bar{x},0^+,p) - \overline{v}^*(\bar{x},0^-,p)]
\end{aligned} \tag{62}$$

which satisfy following single-value conditions

$$\int_{-1}^{1}\varphi_1^*(s,p)ds = 0, \quad \int_{-1}^{1}\varphi_2^*(s,p)ds = 0 \tag{63}$$

Using Eq. (42), the field expressions (52,) (53), (59), (60) and the mechanical boundary conditions (33), (34), (36) and (37) in the *time*-plane, unknown functions $C_j(j=1,\cdots,8)$ can be expressed in term of $\varphi_1^*(\bar{x},p)$, $\varphi_2^*(\bar{x},p)$ as

$$C_j(\omega,p) = (-1)^{1+j}\left[(G_1+F_1)\frac{D_{1j}}{D} - (G_2+F_2)\frac{D_{2j}}{D} + G_3\frac{D_{3j}}{D} - G_4\frac{D_{4j}}{D}\right] \tag{64}$$

where D is the determinant and $D_{ij}(i,j=1,\cdots,8)$is the sub-determinant (corresponding to the elimination of the ith row and jth column) of matrix of the system of linear algebraic equations given in Appendix A. F_1, F_2 are given by

$$\begin{aligned}
F_1(\omega,p) &= \frac{i}{2\pi\omega}\int_{-1}^{1}\varphi_1^*(\bar{x},p)e^{i\omega\bar{x}}d\bar{x}\\
F_2(\omega,p) &= \frac{i}{2\pi\omega}\int_{-1}^{1}\varphi_2^*(\bar{x},p)e^{i\omega\bar{x}}d\bar{x}
\end{aligned} \tag{65}$$

Considering the boundary condition (35), the problem can be reduced to two integral equations, which can be written as

$$\begin{aligned}
\lim_{\bar{y}\to 0^-}\left\{\int_{-1}^{1}\sum_{j=1}^{2}k_{1j}(\bar{x},\bar{y},\eta,p)\varphi_j^*(\eta,p)d\eta\right\} &= 2\pi\cdot\omega_1^T(\bar{x},p)\\
\lim_{\bar{y}\to 0^-}\left\{\int_{-1}^{1}\sum_{j=1}^{2}k_{2j}(\bar{x},\bar{y},\eta,p)\varphi_j^*(\eta,p)d\eta\right\} &= 2\pi\cdot\omega_2^T(\bar{x},p)
\end{aligned} \tag{66}$$

where $\omega_1^T(\bar{x},p)$ and $\omega_2^T(\bar{x},p)$ are crack surface equivalent tangential and normal stresses caused by the temperature, which are given by

$$\omega_1^T(\bar{x},p)=\int_{-\infty}^{\infty}\sum_{j=1}^{8}(-1)^j\left(r_1\frac{D_{j5}}{D}-r_2\frac{D_{j6}}{D}+r_3\frac{D_{j7}}{D}-r_4\frac{D_{j8}}{D}\right)G_j e^{-i\omega\bar{x}}d\omega - \int_{-\infty}^{\infty}\sum_{j=1}^{2}B_j t_j e^{-i\omega\bar{x}}d\omega \quad (67)$$

$$\omega_2^T(\bar{x},p)=\int_{-\infty}^{\infty}\sum_{j=1}^{8}(-1)^j\left(p_1\frac{D_{j5}}{D}-p_2\frac{D_{j6}}{D}+p_3\frac{D_{j7}}{D}-p_4\frac{D_{j8}}{D}\right)G_j e^{-i\omega\bar{x}}d\omega - \int_{-\infty}^{\infty}\sum_{j=1}^{2}B_j q_j e^{-i\omega\bar{x}}d\omega \quad (68)$$

and the kernels of the equations are given as

$$k_{ij}(\bar{x},\bar{y},\eta,p)=\begin{cases}\int_0^{\infty}K_{ij}(\omega,\bar{y},p)\sin(\omega(\eta-\bar{x}))d\omega,(i=j)\\ \int_0^{\infty}K_{ij}(\omega,\bar{y},p)\cos(\omega(\eta-\bar{x}))d\omega,(i\neq j)\end{cases},\quad (i,j=1,2) \quad (69)$$

where $K_{ij}(\omega,\bar{y},p)$ $(i,j=1,2)$ are given in Appendix A. The singular nature of the kernels $k_{ij}(i,j=1,2)$ can be determined by examining the asymptotic behavior of K_{ij} as ω approaches to infinity

$$K_{ij}^{(\infty)}(\omega,0,p)=a_{ij}^{(0)}+\frac{a_{ij}^{(1)}}{\omega}+\frac{a_{ij}^{(2)}}{\omega^2}+\frac{a_{ij}^{(3)}}{\omega^3}+\cdots+\frac{a_{ij}^{(9)}}{\omega^9}+O(\frac{1}{\omega^{10}})\quad (i,j=1,2) \quad (70)$$

where the superscript (∞) stands for the asymptotic expansion as $\omega\to\infty$, $a_{ij}^{(m)}(i,j=1,2,m=0,1,2,\cdots,9)$ are longthy functions of thermalelastical parameters and p, and they are not reproduced here. In the numerical process, these parameters and p are constants, it is very easy to give the values of $a_{ij}^{(m)}$. We note that the leading terms $a_{11}^{(0)}=\chi_1$, $a_{12}^{(0)}=0$, $a_{21}^{(0)}=0$, $a_{22}^{(0)}=\chi_2$.

Extracting the singular terms by using Eq. (70), Eq. (66) is rearranged as

$$\begin{aligned}&\int_{-1}^{1}\left\{\left[\frac{\chi_1}{\eta-\bar{x}}+H_{11}(\bar{x},\eta,p)\right]\varphi_1^*(\eta,p)+H_{12}(\bar{x},\eta,p)\varphi_2^*(\eta,p)\right\}d\eta=2\pi\cdot\omega_1^T(\bar{x},p)\\ &\int_{-1}^{1}\left\{H_{21}(\bar{x},\eta,p)\varphi_1^*(\eta,p)+\left[\frac{\chi_2}{\eta-\bar{x}}+H_{22}(\bar{x},\eta,p)\right]\varphi_2^*(\eta,p)\right\}d\eta=2\pi\cdot\omega_2^T(\bar{x},p)\end{aligned} \quad (71)$$

with

$$H_{ij}(\bar{x},\eta,p)=\int_0^{L_{ij}}\left(K_{ij}^{(\infty)}(\omega,0,p)-a_{ij}^{(0)}-\frac{a_{ij}^{(1)}}{\omega}\right)\sin[\omega(\eta-\bar{x})]d\omega+$$
$$\int_{L_{ij}}^{\infty}\left(K(\omega,0,p)-K_{ij}^{(\infty)}(\omega,0,p)\right)\sin[\omega(\eta-\bar{x})]d\omega+$$
$$\int_{L_{ij}}^{\infty}\left(K_{ij}^{(\infty)}(\omega,0,p)-a_{ij}^{(0)}-\frac{a_{ij}^{(1)}}{\omega}\right)\sin[\omega(\eta-\bar{x})]d\omega+$$
$$\frac{\pi}{2}a_{ij}^{(1)}sign(\eta-\bar{x}),\quad (i=j) \tag{72}$$

$$H_{ij}(\bar{x},\eta,p)=\int_0^{L_{ij}}\left(K_{ij}^{(\infty)}(\omega,0,p)\right)\cos[\omega(\eta-\bar{x})]d\omega+$$
$$\int_{L_{ij}}^{\infty}\left(K(\omega,0,p)-K_{ij}^{(\infty)}(\omega,0,p)\right)\cos[\omega(\eta-\bar{x})]d\omega+$$
$$\int_{L_{ij}}^{\infty}\left(K_{ij}^{(\infty)}(\omega,0,p)-\frac{a_{ij}^{(1)}}{\omega}\right)\cos[\omega(\eta-\bar{x})]d\omega-$$
$$a_{ij}^{(1)}\left[\gamma_0+\int_0^{L_{ij}|\eta-\bar{x}|}\frac{\cos\alpha-1}{\alpha}d\alpha+In(L_{ij}|\eta-\bar{x}|)\right],\quad (i\neq j) \tag{73}$$

where $sign(\cdot)$ is signal function, γ_0 = 0.57721566490 is the Euler's constant, $L_{ij}(i,j=1,2)$ are integration cut-off points, which are arbitrary positive real numbers and can be determined appropriately in numerical process. The first integral in the right hand sides of Eqs. (70) and (71) can be computed numerically using Gauss-Quadrature technique. The second integral in the right hand sides of Eqs. (70) and (71) become negligible [Dag (2001)] when $L_{ij}(i,j=1,2)$ reach sufficiently large. The third integral in the right hand sides of Eqs. (70) and (71) can be evaluated in closed form, the formulae used to compute this type integral are given in Appendix B.

Similar to the temperature problem, the solution of Eq. (71) can be expressed as

$$\varphi_1^*(\eta,p)=\frac{\psi_1^*(\eta,p)}{\sqrt{1-\eta^2}},\quad \psi_1^*(\eta,p)=\sum_{n=1}^{N}b_nT_n(\eta)$$
$$\varphi_2^*(\eta,p)=\frac{\psi_2^*(\eta,p)}{\sqrt{1-\eta^2}},\quad \psi_2^*(\eta,p)=\sum_{n=1}^{N}c_nT_n(\eta) \tag{74}$$

Eq. (71) and single-value conditions (63) can be converted into a system of linear

equations of $2N \times 2N$

$$\begin{aligned}
&\sum_{l=1}^{N}\left[\left(\frac{\chi_1}{\zeta_l-\tau_m}+H_{11}(\tau_m,\zeta_l,p)\right)\frac{\psi_1^*(\zeta_l,p)}{N}+H_{12}(\tau_m,\zeta_l,p)\frac{\psi_2^*(\zeta_l,p)}{N}\right]\\
&=2\pi\cdot\omega_1^T(\tau_m,p)\\
&\sum_{l=1}^{N}\left[H_{21}(\tau_m,\zeta_l,p)\frac{\psi_1^*(\zeta_l,p)}{N}+\left(\frac{\chi_2}{\zeta_l-\tau_m}+H_{22}(\tau_m,\zeta_l,p)\right)\frac{\psi_2^*(\zeta_l,p)}{N}\right]\\
&=2\pi\cdot\omega_2^T(\tau_m,p)
\end{aligned} \tag{75}$$

$$\sum_{l=1}^{N}\frac{\pi\cdot\psi_1^*(\zeta_l,p)}{N}=0,\quad \sum_{l=1}^{N}\frac{\pi\cdot\psi_2^*(\zeta_l,p)}{N}=0 \tag{76}$$

where

$$\zeta_l=\cos(\frac{2l-1}{2N}\pi)\quad(l=1,\cdots,N),\quad \tau_m=\cos(\frac{m}{N}\pi)\quad(m=1,\cdots,N-1) \tag{77}$$

The stress intensity factors in the Laplace domain defined as

$$\begin{aligned}
K_I^*(1)&=\lim_{\bar{x}\to1^+}\sqrt{2(\bar{x}-1)}\sigma_{yy}^*(\bar{x},0,p)=-\frac{\chi_2}{2}\varphi_2^*(1,p),\\
K_I^*(-1)&=\lim_{\bar{x}\to1^-}\sqrt{2(-1-\bar{x})}\overline{\sigma}_{yy}^*(\bar{x},0,p)=\frac{\chi_2}{2}\varphi_2^*(-1,p),\\
K_{II}^*(1)&=\lim_{\bar{x}\to1^+}\sqrt{2(\bar{x}-1)}\overline{\sigma}_{xy}^*(\bar{x},0,p)=-\frac{\chi_1}{2}\varphi_1^*(1,p),\\
K_{II}^*(-1)&=\lim_{\bar{x}\to1^-}\sqrt{2(-1-\bar{x})}\overline{\sigma}_{xy}^*(\bar{x},0,p)=\frac{\chi_1}{2}\varphi_1^*(-1,p)
\end{aligned} \tag{78}$$

The numerical Laplace inversion of (78) is conducted numerically by the method provided by Miller and Guy (1966).

5 Numerical results and discussion

To conduct the foregoing analysis, numerical parameters of heat conduction and shape are presented as follows

$$H_a=1,\ H_b=1,\ T_a=0,\ T_b=1,\qquad f_b(\bar{x})=\begin{cases}1-\frac{\bar{x}^2}{\overline{x_0}^2}, & |\bar{x}|\le\overline{x_0}\\ 0, & |\bar{x}|>\overline{x_0}\end{cases} \tag{79}$$

where H_a, H_b are defined as in Eq. (23), $\overline{x_0}$ stands for half of the dimensionless heating length. We assume the strip is heated from the upper surface by the surrounding

media. The numerical results of temperature distribution along the crack surfaces and extended line and transient thermal stress intensity factors are analyzed.

To verify the validity of present work, firstly let us restrict our attention to the dimensionless thermal resistant Bi for $Bi \to 0$ with $H_a, H_b \to \infty$. This transient problem with an insulated crack under constant temperature distribution on the boundary was investigated by Zhou, Li, and Qin (2007). By comparison from Figure 2 and Figure 3, it can be found that the present results are coincident very well with those of Zhou, Li, and Qin (2007).

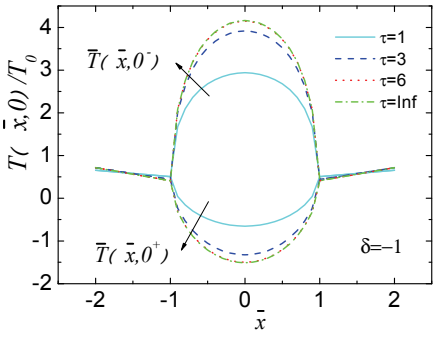

Figure 2: Normalized temperature $\overline{T}(\bar{x},0^+)$ and $\overline{T}(\bar{x},0^-)$ along an insulated crack surface and extended line.

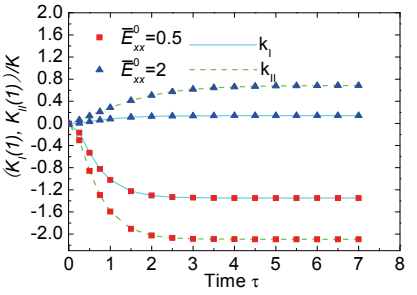

Figure 3: The variation of normalized transient thermal stress intensity factors at an insulated crack tip with dimensionless time τ, $\beta = -1$, $\delta = 1$, $\gamma = 0$.

5.1 Temperature field

Figure 4(a) and 4(b) show the distribution of the temperature along the crack surfaces and the crack extended line with the change of dimensionless time τ when $\delta = 1$ or 2,$Bi = 1$,$\bar{a} = \bar{b} = 1$ and $\bar{k}_{10} = 2$. Here *Inf* stands for infinity(∞). As shown in Figure 4, the temperature rises as the time proceeds and reaches the steady state at $\tau \approx 4.5$ for $\delta = 1$, at $\tau \approx 4$ for $\delta = 2$. Figure 4 also indicates the temperature jump across the crack surfaces becomes more pronounced as the values of δ decrease.

Figure 5(a) and 5(b) show the distribution of the temperature along the crack surfaces and the crack extended line with different values of dimensionless thermal resistant Bi in the steady state when $\delta = 1$ or 2,$\bar{a} = \bar{b} = 1$ and $\bar{k}_{10} = 2$. Here *Inf* also stands for infinity (∞). As expected, the temperature jump across the crack surfaces becomes more pronounced as the dimensionless thermal resistant Bi de-

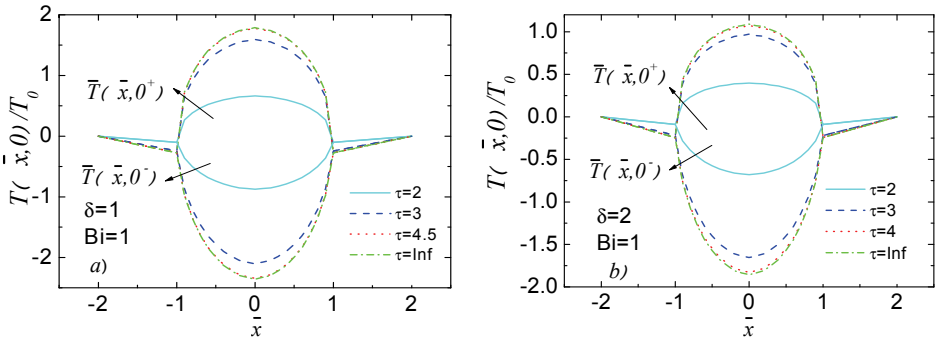

Figure 4: Variation of the normalized temperatures $\overline{T}(\bar{x},0^+)$ and $\overline{T}(\bar{x},0^-)$ on the crack surfaces and crack extended line $(\bar{y}=0)$ with dimensionless time τ, $Bi=1$, $\bar{a}=\bar{b}=1$, $\bar{k}_{10}=2$. (a) $\delta=1$, (b) $\delta=2$.

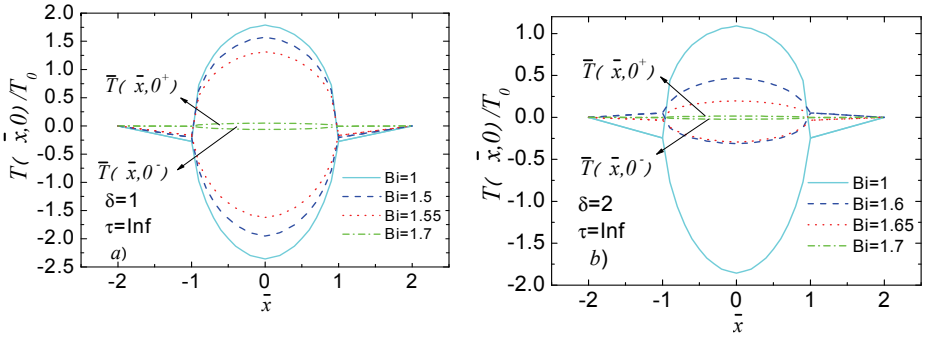

Figure 5: Influence of dimensionless thermal resistant Bi on the normalized temperatures $\overline{T}(\bar{x},0^+)$ and $\overline{T}(\bar{x},0^-)$ on the crack surfaces and crack extended line $(\bar{y}=0)$ in the steady state, $\bar{a}=\bar{b}=1$,$\bar{k}_{10}=2$. (a) $\delta=1$, (b) $\delta=2$.

creases, i.e. the crack region thermal resistant $(Bi=c/k_{y1}/R_c)$ increases. Figure 5 also indicates the temperature jump across the crack surfaces becomes more pronounced as the values of δ decrease.

The temperature on the crack surfaces and the crack extended line with different relative distance $\bar{b}$ of the crack from the heated region is showed in Figure 6. Here *inf* represents infinity $(+\infty)$. Temperature jump across the crack surfaces increases when the crack becomes closer to the heated region.

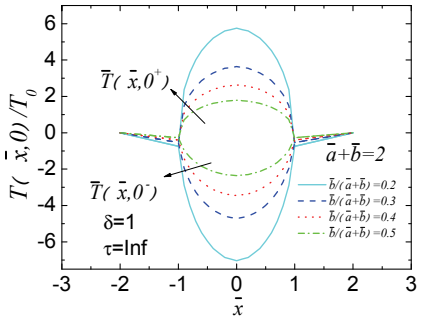

Figure 6: Influence of the relative distance $\overline{b}$ of the crack from the heated region on the normalized temperatures $\overline{T}(\overline{x},0^+)$ and $\overline{T}(\overline{x},0^-)$ on the crack surfaces and crack extended line $(\overline{y}=0)$ in the steady state, $\delta=1$,$Bi=1$,$\overline{k}_{10}=2$.

5.2 Stress intensity factors

The orthotropic and nonhomogeneous parameter adopted for the numerical calculations of transient normalized stress intensity factors (SIFs) are shown in table 1 [Ootaot (2005)].

Table 1: Orthotropic and nonhomogeneous parameters

$2l/c$	δ	γ	β	$\overline{E}^0_{xx}$	$\overline{E}^0_{yy}$	$\overline{G}^0_{xy}$	$\overline{\alpha}^0_{xx}$	$\overline{\alpha}^0_{yy}$	$\overline{k}_{10}$
Case 1	1	0	1	0.5	1	1	1	1	1
	1	0	1	2	1	1	1	1	1
	1	0	-1	0.5	1	1	1	1	1
	1	0	-1	2	1	1	1	1	1
Case 2	1	1	0.01	1.01	1	1	0.5	1	1
	1	1	0.01	1.01	1	1	2	1	1
	1	-1	0.01	1.01	1	1	0.5	1	1
	1	-1	0.01	1.01	1	1	2	1	1
Case 3	1	0	0.01	1.01	1	1	1	1	0.5
	1	0	0.01	1.01	1	1	1	1	2
	-1	0	0.01	1.01	1	1	1	1	0.5
	-1	0	0.01	1.01	1	1	1	1	2

Figure 7(a) and 7(b) illustrate the effect of the stiffness parameter β and $\overline{E}^0_{xx}$ (Case 1) on the mode I and II transient normalized stress intensity factors (SIFs) $(K_I,K_{II})/K$ $(K=\alpha_0 E_0 T_0\sqrt{c})$ with different dimensionless time τ. It can be seen SIFs vary with

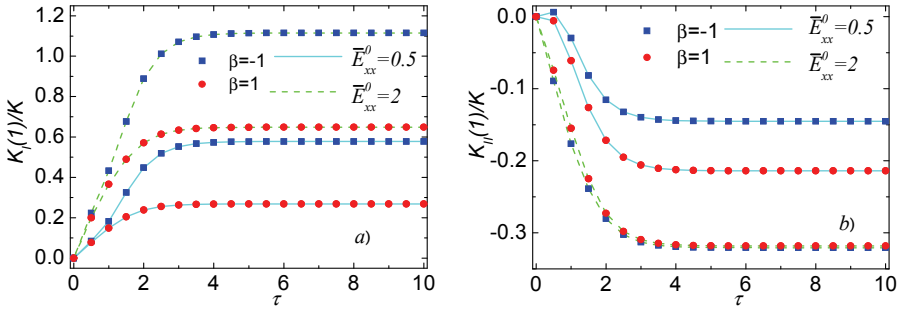

Figure 7: Variation of normalized stress intensity factors with dimensionless time τ for different stiffness parameter β and $\overline{E}^0_{xx}$ (Case 1),$\overline{a}=\overline{b}=1$,$Bi=0.1$. (a) Mode I, (b) Mode II

the time from their initial zero value to a steady state. The time that SIFs reach the steady state is $\tau\approx 3$ for mode I and $\tau\approx 4$ for mode II SIF when $\beta=1$; $\tau\approx 4$ for both mode I and II SIFs when $\beta=-1$. As shown in Figure 7(a) mode I SIF decreases with the increasing of the stiffness parameter β, increases with the increasing of $\overline{E}^0_{xx}$. As illustrated in Figure 7(b), mode II SIF increases with the increasing of $\overline{E}^0_{xx}$ for either $\beta=1$ or $\beta=-1$.

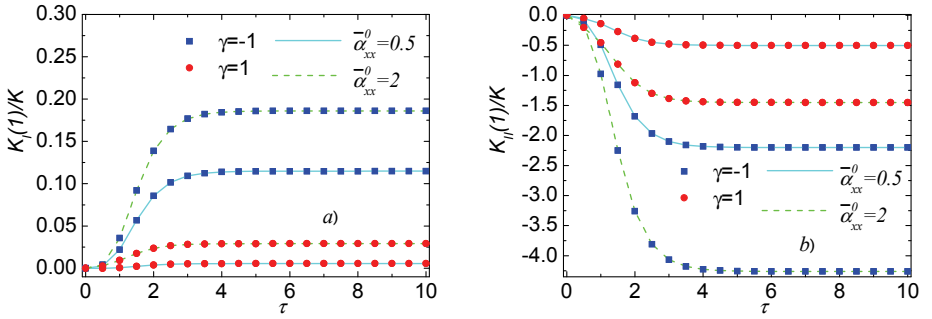

Figure 8: Variation of normalized stress intensity factors with dimensionless time τ for different thermal expansion parameter γ and $\overline{\alpha}^0_{xx}$(Case 2),$\overline{a}=\overline{b}=1$,$Bi=0.1$. (a) Mode I, (b) Mode II

Figure 8(a) and 8(b) illustrate the effect of the thermal expansion parameter γ and $\overline{\alpha}^0_{xx}$ (Case 2) on the mode I and II transient normalized stress intensity factors (SIFs) $(K_I,K_{II})/K$ $(K=\alpha_0E_0T_0\sqrt{c})$ with different dimensionless time τ. It can be seen SIFs increase with the time from their initial zero value to the maximum value at

a steady state. The time that SIFs reach the steady state is $\tau \approx 3$ for mode I and $\tau \approx 4$ for mode II SIF when $\gamma = 1$; $\tau \approx 4$ for both mode I and II SIFs when $\gamma = -1$. It may be obtained the absolute values of mode I and II SIFs in a transient state increase when the thermal expansion parameter γ decreases from Figure 8(a) or $\overline{\alpha}_{xx}^{0}$ increases from Figure 8(b).

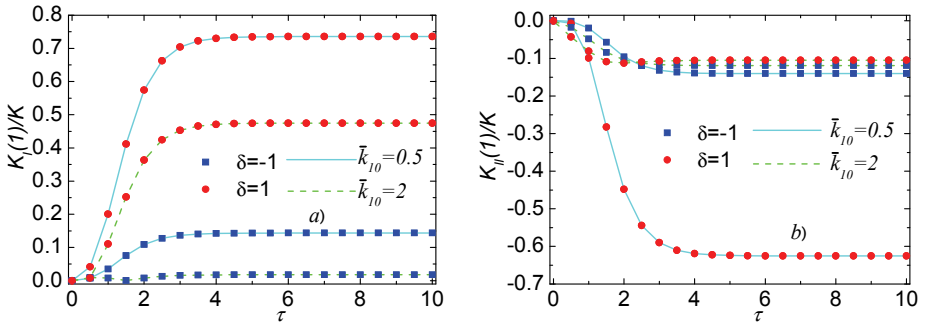

Figure 9: Variation of normalized stress intensity factors with dimensionless time τ for different thermal conductivity parameter δ and $\overline{k}_{10}$ (Case 3),$\overline{a} = \overline{b} = 1, Bi = 0.1$. (a) Mode I, (b) Mode II

Figure 9(a) and 9(b) show the influence of the thermal conductivity parameter δ and $\overline{k}_{10}$ (Case 3) on the mode I and II transient normalized stress intensity factors (SIFs) $(K_I, K_{II})/K$ $(K = \alpha_0 E_0 T_0 \sqrt{c})$ with different dimensionless time τ. It can be seen SIFs rise as the time proceeds and are greatest at a steady state. Both mode I SIF and mode II SIF reach the steady state at $\tau \approx 4$ for either $\gamma = 1$ or $\gamma = -1$. From Figure 9(a), it may be obtained mode I SIF in a transient state increases when the thermal conductivity parameter δ increases or $\overline{k}_{10}$ decreases. From Figure 9(b), it may be obtained with the parameter δ increasing the absolute values of mode II SIF in a transient state increase when $\overline{k}_{10} = 0.5 < 1$, while decrease when $\overline{k}_{10} = 2 > 1$.

Figure 10(a) and 10(b) show the influence of the relative distance $\overline{b}$ of the crack from the heated region on the mode I and II transient normalized stress intensity factors (SIFs) $(K_I, K_{II})/K$ $(K = \alpha_0 E_0 T_0 \sqrt{c})$ with different dimensionless time τ. It can be seen that both mode I SIF and mode II SIF reach the steady state at $\tau \approx 4$. Figure 10(a) and 10(b), the absolute values of both mode I SIF and mode II SIF in a transient state increase when the crack is close to the heated region.

Figure 11(a) and11(b) show the influence of the dimensionless thermal resistant Bi on the mode I and II transient normalized stress intensity factors (SIFs) $(K_I, K_{II})/K$ $(K = \alpha_0 E_0 T_0 \sqrt{c})$ with different dimensionless time τ. It can be seen that both mode I SIF and mode II SIF reach the steady state at $\tau \approx 4$. As expected, the absolute

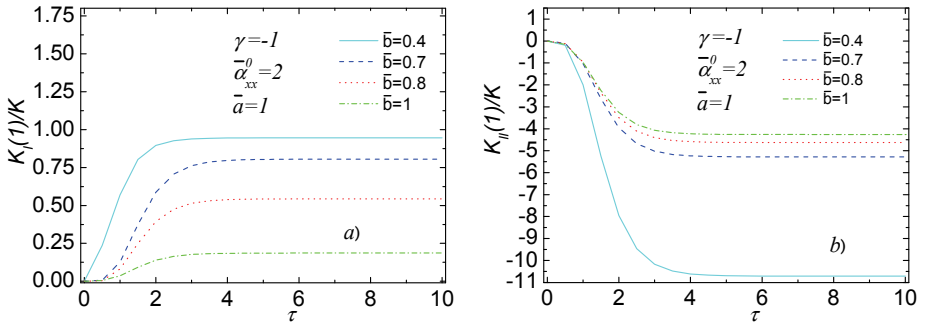

Figure 10: Variation of normalized stress intensity factors with dimensionless time τ for different relative distance $\overline{b}$ of the crack from the heated region, $\gamma = -1$, $\overline{\alpha}^{0}_{xx} = 2$,$Bi = 0.1$. (a) Mode I, (b) Mode II

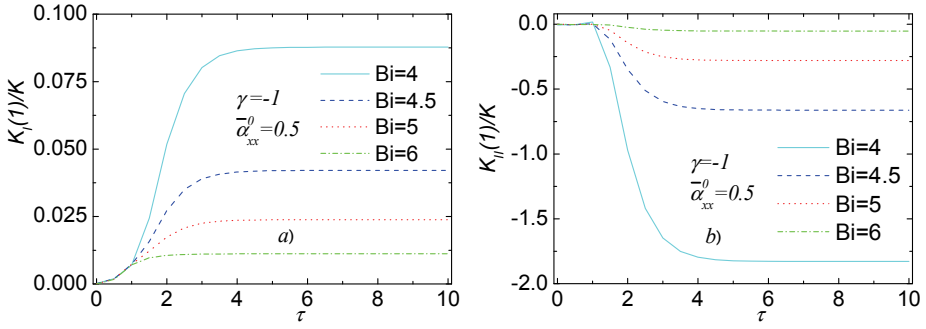

Figure 11: Variation of normalized stress intensity factors with dimensionless time τ for different dimensionless thermal resistant Bi, $\gamma = -1$, $\overline{\alpha}^{0}_{xx} = 0.5$, $\overline{a} = \overline{b} = 1$. (a) Mode I, (b) Mode II

values of both mode I SIF and mode II SIF in a transient state increase as the value of dimensionless thermal resistant Bi decrease, i.e. the crack region thermal resistant ($Bi = c/k_{y1}/R_c$) increases.

6 Conclusions

In this paper, the singular integral equation method has been applied to study the transient response of an orthotropic functionally graded strip with a partially insulated crack under convective heat transfer supply. The considered problem is finally

reduced to solving a system of Cauchy type singular integral equations via Laplace transform and Fourier transform. The asymptotic expansions with high order terms for the singular integral kernel are considered in the numerical analysis. Numerical inversion of Laplace transform is conducted.

It has been shown: (i) the temperatures along the crack surfaces and crack extended line and transient thermal SIFs rise as the time proceeds and reach the steady state at certain time; (ii) The orthotropic parameters, material nonhomogeneous parameters and dimensionless thermal resistant do influence the temperature distribution and the transient thermal SIFs; (iii) The crack growth and thermal fracture behavior of orthotropic graded mediums can be controlled by optimizing the gradation profiles of the material properties.

Acknowledgement: This work was supported by The National Basic Research Program of China (2005CB321701), the National Natural Science Foundation of China (No. 10531080), the National Natural Science Foundation of China (No. 10661009), the National Basic Research Program (973) of China (2008617613) and the Science Foundation for the Postdoctoral Program.

References

Chen, J. (2005): Determination of thermal stress intensity factors for an interface crack in a graded orthotropic coating-substrate structure. *International Journal of Fracture*, vol. 133, pp. 303–328.

Chen, J.; Liu, Z. (2005): Transient response of a mode III crack in an orthotropic functionally graded strip. *European Journal of Mechanics A/Solids*, vol. 24, pp. 325–336.

Chen, J.; Liu, Z.; Zou, Z. (2002): Transient internal crack problem for a nonhomogeneous orthotropic strip (mode I). *International Journal of Engineering Science*, vol. 40, pp. 1761–1774.

Chen, J.; Soh, A.; Liu, J.; Liu, Z. (2004): Thermal fracture analysis of a functionally graded orthotropic strip with a crack, *International Journal of Mechanics and Design*, vol. 1, pp. 131–141.

Ching, H. K.; Chen, J. K. (2006): Thermomechanical analysis of functionally graded composites under laser heating by the MLPG method. *CMES: Computer Modeling in Engineering & Sciences*, vol.13, no. 3, pp.199-217.

Dag, S. (2001): *Crack and contact problem in graded materials*. Ph. D. Dissertation, Lehigh University.

Dag, S. (2006): Thermal fracture analysis of orthotropic functionally graded mate-

rials using an equivalent domain integral approach. *Engineering Fracture Mechanics,* vol. 73, pp. 2802–2828.

Dag, S.; Yildirim, B.; Erdogan, F. (2004): Interface Crack Problems in Graded Orthotropic Medium: Analytical and Computational Approaches. *International Journal of Fracture*, vol. 130, pp. 471-496.

El-Borgi, S.; Erdogan, F.; Hatira, F. (2003): Stress intensity factors for an interface crack between a functionally graded coating and a homogeneous substrate. *International Journal of Fracture*, vol. 123, pp. 139–162.

El-Borgi, S.; Erdogan, F.; Hidri, L. (2004): A partially insulated crack embedded in an infinite functionally graded medium under thermo-mechanical loading. *International Journal of Engineering Science*, vol. 42, pp. 371–393.

Gu, P.; Asaro, RJ. (1997): Cracks in functionally graded materials. *International Journal of Solids and Structure,* vol. 34, no. 1, pp. 1–17.

Guo, L.; Noda, N.; Wu, L. (2008): Thermal fracture model for a functionally graded plate with a crack normal to the surfaces and arbitrary thermomechanical properties. *Composites Science and Technology*, vol. 68, pp. 1034–1041.

Guo, L.; Wu, L.; Zeng, T.; Ma, L. (2004): Mode I crack problem for a functionally graded orthotropic strip. *European Journal of Mechanics A/Solids,* vol. 23, pp. 219–234.

Han, F.; Pan, E.; Roy, A. K.; Yue, Z. (2006): Responses of piezoelectric, transversaly isotropic, functionally graded and multilayered half spaces to uniform circular surface loading. *CMES: Computer Modeling in Engineering & Sciences*, vol. 14, pp.15-30.

Itou, S. (2004): Thermal stresses around a crack in the nonhomogeneous interfacial layer between two dissimilar elastic half-planes. *.International Journal of Solids and Structures*, vol. 41, pp. 923–945.

Jin, Z.; Batra, R. (1996): Stress intensity relaxation at the tip of an edge crack in a functionally graded material subjected to a thermal shock. *Journal of Thermal Stresses,* vol. 19, pp. 317–339.

Jin, Z.; Feng, Y. (2008): Thermal fracture resistance of a functionally graded coating with periodic edge cracks. *Surface & Coatings Technology,* vol. 202, pp. 4189–4197.

Jin, Z; Noda, N. (1994): Edge crack in a nonhomogeneous half plane under thermal loading. *Journal of thermal stresses*, vol. 17, pp. 591-599.

Jin, Z.; Noda, N. (1994): Transient thermal stress intensity factors for a crack in a semi-infinite plane of a functionally gradient material. *International Journal of Solids and Structures,* vol. 31, pp. 203–218.

Jin, Z.; Paulino, G. (2001): Transient thermal stress analysis of an edge crack in a functionally graded material. *International Journal of Fracture,* vol. 107, pp. 73–98.

Kaysser, WA.; Ilschner, B. (1995): FGM research activities in Europe. *MRS Bull*, vol. 20, no. 1. pp. 22–26.

Kim, J.; Paulino, G. (2002): Mixed-mode fracture of orthotropic functionally graded materials using finite elements and the modified crack closure method. *Engineering Fracture Mechanics,* vol. 69, pp. 1557–1586.

Li,X. (2008): *Integral equation*. Science Press, Beijing.

Liu, D.; Yu, D. (2008): The coupling method of natural boundary element and mixed finite element for stationary Navier-Stokes equation in unbounded domains. *CMES: Computer Modeling in Engineering & Sciences*, vol. 37, no. 3, pp. 305-329.

Liu, D.; Zheng, X.; Liu, Y. (2009): A discontinuous galerkin finite element method for heat conduction problems with local high gradient and thermal contact resistance. *CMES: Computer Modeling in Engineering & Sciences*, vol. 39, no. 3, pp. 263-299.

Liu, K.; Long, S.; Li, G. (2008): A meshless local petrov-galerkin method for the analysis of cracks in the isotropic functionally graded material. *CMC: Computers Materials & Continua*, vol. 7, no. 1, pp. 43–57.

Miller, M.; Guy, M. (1966): Numerical inversion of the Laplace transform by the use of Jacobi polynomials, *SIAM Journal of Numerical Analysis*, vol. 3, pp. 624–635.

Minutolo, V.; Ruocco, E. Ciaramella, S. (2009): Isoparametric FEM vs. BEM for elastic functionally graded materials. *CMES: Computer Modeling in Engineering & Sciences*, vol. 41, no.1, pp. 27-48.

Miyamoto, Y.; Kaysser, W.; Rabin, B.; Kawasaki, A.; Ford, R. (1999): *Functionally graded materials: design, processing and applications*. Kluwer Academic Publishers, Dordrecht.

Nino, M.; Hirai, T.; Watanabe, R. (1987): The functionally gradient materials. *Journal of Japan Society of Composite Materials,* vol.13, pp. 257-264.

Noda, N. (1999): Thermal stresses in functionally graded materials. *Journal of Thermal Stresses*, vol. 22, no. 1, pp. 477–512.

Noda, N.; Jin, Z. (1993): Thermal stress intensity factors for a crack in a functionally gradient material. *International Journal of Solids and Structure,* vol, 30, pp. 1039-56.

Noda, N.; Jin, Z. (1994): A crack in a functionally gradient material under thermal

shock. *Archive of Applied Mechanic,* vol. 64, pp. 99- 110.

Ootao, Y.; Tanigawa, Y. (2005): Transient thermal stresses of orthotropic functionally Graded thick strip due to nonuniform heat supply. *Structure Engineering and Mechanics*, vol. 20, pp. 559–573.

Ootao, Y; Tanigawa, Y. (2006): Transient thermoelastic analysis for a functionally graded hollow cylinder. *Journal of Thermal Stresses*, vol. 29, pp. 1031–1046.

Oyekoya, O.; Mba, D.; **El-Zafrany, A.** (2008): Structural Integrity of Functionally Graded Composite Structure using Mindlin-type Element. *CMES: Computer Modeling in Engineering & Sciences*, vol. 34, no. 1, pp.55-85.

Ozturk, M.; Erdogan, F. (1997): Mode I Crack Problem in an Inhomogeneous Orthotropic Medium. *International Journal of Engineering Science*, vol. 35, pp. 869–883.

Ozturk, M.; Erdogan, F. (1999): The Mixed Mode Crack Problem in an Inhomogeneous Orthotropic Medium. *International Journal of Fracture*, vol. 98, pp. 243–261.

Sethuraman, R.; Rajesh, N. (2009): Evaluation of elastic-plastic crack tip parameters using partition of unity finite element method and pseudo elastic analysis. *CMES: Computer Modeling in Engineering & Sciences*, vol. 39, no. 1, pp. 67-99.

Shin, S.; Huang, C.; Shiah, Y. (2009): Study of the underfill effect on the thermal fatigue life of WLCSP-Experiments and finite element simulations. *CMES: Computer Modeling in Engineering & Sciences*, vol. 40, no. 1, pp. 83-103.

Sladek, J.; Sladek, V.; Krivacek, J. (2005): Meshless local petrov-galerkin method for stress and crack analysis in 3-d axisymmetric FGM bodies. *CMES: Computer Modeling in Engineering & Sciences*, vol. 8, no. 3, pp. 259–270.

Sladek, J.; Sladek, V.; Solek, P.; Wen, P. H.; Atluri, S. N. (2008): Thermal analysis of Reissner-Mindlin shallow shells with FGM properties by the MLPG. *CMES: Computer Modeling in Engineering & Sciences*, vol. 30, no. 2, pp.77-97.

Sladek, J.; Sladek, V.; Tan, C.; Atluri, S. N. (2008): Analysis of transient heat conduction in 3D anisotropic functionally graded solids by the MLPG. *CMES: Computer Modeling in Engineering & Sciences*, vol. 32, no. 3, pp. 161-174.

Sladek, J.; Sladek, V.; Zhang, Ch. (2003): Application of meshless local Petrov-Galerkin (MLPG) method to elastodynamic problems in continuously nonhomogeneous solids. *CMES: Computer Modeling in Engineering & Sciences*, vol. 4, pp. 637-648.

Sladek, J.; Sladek, V.; Zhang, Ch. (2005): The MLPG method for crack analysis in anisotropic functionally graded materials. *In Structural Integrity & Durability*, Vol. 1, pp. 131-143.

Sladek, J.; Sladek, V.; Zhang, Ch. (2007): Fracture analyses in continuously nonhomogeneous piezoelectric solids by the MLPG. *CMES: Computer Modeling in Engineering & Sciences*, vol. 19, no. 3, pp. 247–262.

Suresh, S.; Mortensen, A. (1998): *Fundamentals of functionally graded materials*. IOM Communications Ltd, London.

Walters, M; Paulino, G; Dodds Jr, R. (2004): Stress-intensity factors for surface cracks in functionally graded materials under mode-I thermomechanical loading. *International Journal of Solids and Structures*, vol. 41, pp. 1081–1118.

Wang, B.; Han, J.; Du, S. (2000): Thermoelastic fracture mechanics for nonhomogeneous Material subjected to unsteady thermal load. *ASME Journal of Applied Mechanics*, vol. 67, pp. 87–95.

Wen, P.; Aliabadi, **M.; Liu, Y.** (2008): Meshless method for crack analysis in functionally graded materials with Enriched Radial Base Functions**.** *CMES: Computer Modeling in Engineering & Sciences*, vol.30, no. 3, pp.133-147.

Yang, X.; Qin, Y.; Zhuang, Z.; You, X. (2008): **I**nvestigation of dynamic fracture behavior in functionally graded materials. *Modeling and Simulation in Materials Science and Engineering*, vol. 16, pp. 1-15.

Yu, D. (1993): *Mathematical Theory of Natural Boundary Element Method.* Science Press, Beijing.

Yu, D. (2002): *Natural Boundary Integrals Method and its Applications*. Kluwer Academic Publishers.

Yu, D.; Huang, H. (2008): The artificial boundary method for a nonlinear interface problem on unbounded domain. *CMES: Computer Modeling in Engineering & Sciences*, vol. 35, no. 3, pp. 227-252.

Zhou, Y.; Li, X.; Qin J. (2007): Transient thermal stress analysis of orthotropic functionally graded materials with a crack. *Journal of Thermal Stresses,* vol. 30, pp. 1211–1231.

Zhou, Y.; Li, X.; Yu, D. (2008): Integral Method for Contact Problem of Bonded Plane Material with Arbitrary Cracks. *CMES: Computer Modeling in Engineering & Sciences*, vol. 36, no. 2, pp. 147-172.

Appendix A: Expressions of some quantities

Expressions of $\Omega_i^{(j)}(i=1,\cdots,4, j=1,2,3)$ appearing in Eq. (42)

$$\Omega_1^{(1)} = \frac{(n_2+H_b)e^{n_2\bar{b}}[n_1(n_2-H_a)e^{n_1\bar{a}} - n_2(n_1-H_a)e^{n_2\bar{a}}]}{\Omega} \tag{80}$$

$$\Omega_1^{(2)} = \frac{H_b\overline{T_b}(n_2-n_1)(n_2-H_a)e^{n_1\bar{a}}}{\Omega} \tag{81}$$

$$\Omega_1^{(3)} = \frac{H_a\overline{T_a}(n_2-n_1)(n_2+H_b)e^{n_2\bar{b}}e^{(n_1+n_2)\bar{a}}}{\Omega} \tag{82}$$

$$\Omega_2^{(1)} = -\frac{(n_1+H_b)e^{n_1\bar{b}}[n_1(n_2-H_a)e^{n_1\bar{a}}-n_2(n_1-H_a)e^{n_2\bar{a}}]}{\Omega} \tag{83}$$

$$\Omega_2^{(2)} = -\frac{H_b\overline{T_b}(n_2-n_1)(n_1-H_a)e^{n_2\bar{a}}}{\Omega} \tag{84}$$

$$\Omega_2^{(3)} = -\frac{H_a\overline{T_a}(n_2-n_1)(n_1+H_b)e^{n_1\bar{b}}e^{(n_1+n_2)\bar{a}}}{\Omega} \tag{85}$$

$$\Omega_3^{(1)} = \frac{(n_2-H_a)e^{n_1\bar{a}}[n_1(n_2+H_b)e^{n_2\bar{b}}-n_2(n_1+H_b)e^{n_1\bar{b}}]}{\Omega} \tag{86}$$

$$\Omega_3^{(2)} = \frac{H_b\overline{T_b}(n_2-n_1)(n_2-H_a)e^{n_1\bar{a}}}{\Omega} \tag{87}$$

$$\Omega_3^{(3)} = \frac{H_a\overline{T_a}(n_2-n_1)(n_2+H_b)e^{n_2\bar{b}}e^{(n_1+n_2)\bar{a}}}{\Omega} \tag{88}$$

$$\Omega_4^{(1)} = -\frac{(n_1-H_a)e^{n_2\bar{a}}[n_1(n_2+H_b)e^{n_2\bar{b}}-n_2(n_1+H_b)e^{n_1\bar{b}}]}{\Omega} \tag{89}$$

$$\Omega_4^{(2)} = -\frac{H_b\overline{T_b}(n_2-n_1)(n_1-H_a)e^{n_2\bar{a}}}{\Omega} \tag{90}$$

$$\Omega_4^{(3)} = -\frac{H_a\overline{T_a}(n_2-n_1)(n_1+H_b)e^{n_1\bar{b}}e^{(n_1+n_2)\bar{a}}}{\Omega} \tag{91}$$

where

$$\Omega = \left[(n_2+H_b)e^{n_2\bar{b}}-(n_1+H_b)e^{n_1\bar{b}}\right]\left[n_1(n_2-H_a)e^{n_1\bar{a}}-n_2(n_1-H_a)e^{n_2\bar{a}}\right]- \left[(n_2-H_a)e^{n_1\bar{a}}-(n_1-H_a)e^{n_2\bar{a}}\right]\left[n_1(n_2+H_b)e^{n_2\bar{b}}-n_2(n_1+H_b)e^{n_1\bar{b}}\right] \tag{92}$$

Expressions of $K(\omega,\bar{y},p)$, K_a and appearing in Eq. (43)

$$K(\omega,\bar{y},p) = \frac{-2}{\omega}\left[n_1\Omega_1^{(1)}e^{n_1\bar{y}}+n_2\Omega_2^{(1)}e^{n_2\bar{y}}\right]-\frac{2Bi}{\omega} \tag{93}$$

$$K_a = \frac{H_a\overline{T_a}(n_2-n_1)e^{(n_1+n_2)\bar{a}}\left[n_1(n_2+H_b)e^{n_2\bar{b}}-n_2(n_1+H_b)e^{n_1\bar{b}}\right]}{\Omega} \tag{94}$$

$$K_b = \frac{H_b \overline{T_b}(n_2 - n_1)\left[n_1(n_2 - H_a)e^{n_1\bar{a}} - n_2(n_1 - H_a)e^{n_2\bar{a}}\right]}{\Omega} \tag{95}$$

Expressions of $a^{(j)}(j = 0, 1, 2, 4, \cdots, 12, 14)$ appearing in Eq. (44)

$$a^{(0)} = \sqrt{\bar{k}_{10}},\ a^{(1)} = -2 \cdot Bi,\ a^{(2)} = \left(\frac{1}{2}p - \frac{1}{8}\delta^2\right)\left(\bar{k}_{10}\right)^{-\frac{1}{2}} \tag{96}$$

$$a^{(4)} = \left(-\frac{1}{8}p^2 + \frac{1}{16}\delta^2 p + \frac{3}{128}\delta^4\right)\left(\bar{k}_{10}\right)^{-\frac{3}{2}} \tag{97}$$

$$a^{(6)} = \left(\frac{1}{16}p^3 - \frac{3}{64}\delta^2 p^2 - \frac{9}{256}\delta^4 p - \frac{5}{1024}\delta^6\right)\left(\bar{k}_{10}\right)^{-\frac{5}{2}} \tag{98}$$

$$a^{(8)} = \left(-\frac{5}{128}p^4 + \frac{5}{128}\delta^2 p^3 + \frac{45}{1024}\delta^4 p^2 + \frac{25}{2048}\delta^6 p + \frac{35}{32768}\delta^8\right)\left(\bar{k}_{10}\right)^{-\frac{7}{2}} \tag{99}$$

$$a^{(10)} = \left(\frac{7}{256}p^5 - \frac{35}{1024}\delta^2 p^4 - \frac{105}{2048}\delta^4 p^3 - \frac{175}{8192}\delta^6 p^2 - \frac{245}{65536}\delta^8 p - \frac{63}{262144}\delta^{10}\right)\left(\bar{k}_{10}\right)^{-\frac{9}{2}} \tag{100}$$

$$a^{(12)} = \left(-\frac{21}{1024}p^6 + \frac{63}{2048}\delta^2 p^5 + \frac{945}{16384}\delta^4 p^4 + \frac{525}{16384}\delta^6 p^3 + \frac{2205}{262144}\delta^8 p^2 + \frac{567}{524288}\delta^{10} p + \frac{231}{4194304}\delta^{12}\right)\left(\bar{k}_{10}\right)^{-\frac{11}{2}} \tag{101}$$

$$a^{(14)} = \left(\frac{33}{2048}p^7 - \frac{231}{8192}\delta^2 p^6 - \frac{2079}{32768}\delta^4 p^5 - \frac{5775}{131072}\delta^6 p^4 - \frac{8085}{524288}\delta^8 p^3 - \frac{6237}{2097152}\delta^{10} p^2 - \frac{2541}{8388608}\delta^{12} p - \frac{429}{33554432}\delta^{14}\right)\left(\bar{k}_{10}\right)^{-\frac{13}{2}} \tag{102}$$

In Eq. (64), D is the determinant and $D_{ij}(i, j = 1, \cdots, 8)$ is the sub-determinant of

the coefficient matrix in the following system:

$$\begin{bmatrix} 1 & 1 & 1 & 1 & -1 & -1 & -1 & -1 \\ s_1 & s_2 & s_3 & s_4 & -s_1 & -s_2 & -s_3 & -s_4 \\ r_1 & r_2 & r_3 & r_4 & -r_1 & -r_2 & -r_3 & -r_4 \\ p_1 & p_2 & p_3 & p_4 & -p_1 & -p_2 & -p_3 & -p_4 \\ 0 & 0 & 0 & 0 & r_1 e^{-m_1\bar{a}} & r_2 e^{-m_2\bar{a}} & r_3 e^{-m_3\bar{a}} & r_4 e^{-m_4\bar{a}} \\ 0 & 0 & 0 & 0 & p_1 e^{-m_1\bar{a}} & p_2 e^{-m_2\bar{a}} & p_3 e^{-m_3\bar{a}} & p_4 e^{-m_4\bar{a}} \\ r_1 e^{m_1\bar{b}} & r_2 e^{m_2\bar{b}} & r_3 e^{m_3\bar{b}} & r_4 e^{m_4\bar{b}} & 0 & 0 & 0 & 0 \\ p_1 e^{m_1\bar{b}} & p_2 e^{m_2\bar{b}} & p_3 e^{m_3\bar{b}} & p_4 e^{m_4\bar{b}} & 0 & 0 & 0 & 0 \end{bmatrix} \cdot \begin{bmatrix} C_1 \\ C_2 \\ C_3 \\ C_4 \\ C_5 \\ C_6 \\ C_7 \\ C_8 \end{bmatrix} = \begin{bmatrix} G_1 + F_1 \\ G_2 + F_2 \\ G_3 \\ G_4 \\ G_5 \\ G_6 \\ G_7 \\ G_8 \end{bmatrix} \tag{103}$$

where

$$G_1(\omega, p) = \frac{i}{2\pi\omega} \frac{A_{11}n_2 - A_{12}n_1}{n_1 - n_2} \int_{-1}^{1} \varphi^*(\bar{x}, p) e^{i\omega\bar{x}} d\bar{x}, \tag{104}$$

$$G_2(\omega, p) = \frac{i}{2\pi\omega} \frac{A_{21}n_2 - A_{22}n_1}{n_1 - n_2} \int_{-1}^{1} \varphi^*(\bar{x}, p) e^{i\omega\bar{x}} d\bar{x} \tag{105}$$

$$G_3(\omega, p) = \frac{i}{2\pi\omega} \frac{t_1 n_2 - t_2 n_1}{n_1 - n_2} \int_{-1}^{1} \varphi^*(\bar{x}, p) e^{i\omega\bar{x}} d\bar{x} \tag{106}$$

$$G_4(\omega, p) = \frac{i}{2\pi\omega} \frac{q_1 n_2 - q_2 n_1}{n_1 - n_2} \int_{-1}^{1} \varphi^*(\bar{x}, p) e^{i\omega\bar{x}} d\bar{x} \tag{107}$$

$$G_5(\omega, p) = \frac{i}{2\pi\omega} \frac{e^{-\bar{a}\gamma}(t_2 - t_1)(e^{n_2\bar{b}} - e^{n_1\bar{b}})}{(n_1 - n_2)\left[e^{n_2(\bar{a}+\bar{b})} - e^{n_1(\bar{a}+\bar{b})}\right]} \int_{-1}^{1} \varphi^*(\bar{x}, p) e^{i\omega\bar{x}} d\bar{x} \tag{108}$$

$$G_6(\omega, p) = \frac{i}{2\pi\omega} \frac{e^{-\bar{a}\gamma}(q_2 - q_1)(n_1 e^{n_2\bar{b}} - n_2 e^{n_1\bar{b}})}{(n_1 - n_2)\left[e^{n_2(\bar{a}+\bar{b})} - e^{n_1(\bar{a}+\bar{b})}\right]} \int_{-1}^{1} \varphi^*(\bar{x}, p) e^{i\omega\bar{x}} d\bar{x} \tag{109}$$

$$G_7(\omega, p) = \frac{i}{2\pi\omega} \frac{(t_2 - t_1) e^{(\gamma + n_1 + n_2)\bar{b}} (n_1 e^{n_1\bar{a}} - n_2 e^{n_2\bar{a}})}{(n_1 - n_2)\left[e^{n_2(\bar{a}+\bar{b})} - e^{n_1(\bar{a}+\bar{b})}\right]} \int_{-1}^{1} \varphi^*(\bar{x}, p) e^{i\omega\bar{x}} d\bar{x} \tag{110}$$

$$G_8(\omega, p) = \frac{i}{2\pi\omega} \frac{(q_2 - q_1) e^{(\gamma + n_1 + n_2)\bar{b}} (n_1 e^{n_1\bar{a}} - n_2 e^{n_2\bar{a}})}{(n_1 - n_2)\left[e^{n_2(\bar{a}+\bar{b})} - e^{n_1(\bar{a}+\bar{b})}\right]} \int_{-1}^{1} \varphi^*(\bar{x}, p) e^{i\omega\bar{x}} d\bar{x} \tag{111}$$

Expressions of quantities appearing in Eq. (69)

$$K_{11}(\omega,\bar{y},p)=\frac{2}{\omega}\left(-r_1\frac{D_{15}}{D}e^{m_1\bar{y}}+r_2\frac{D_{16}}{D}e^{m_2\bar{y}}-r_3\frac{D_{17}}{D}e^{m_3\bar{y}}+r_4\frac{D_{18}}{D}e^{m_4\bar{y}}\right) \tag{112}$$

$$K_{12}(\omega,\bar{y},p)=\frac{2i}{\omega}\left(-r_1\frac{D_{25}}{D}e^{m_1\bar{y}}+r_2\frac{D_{26}}{D}e^{m_2\bar{y}}-r_3\frac{D_{27}}{D}e^{m_3\bar{y}}+r_4\frac{D_{28}}{D}e^{m_4\bar{y}}\right) \tag{113}$$

$$K_{21}(\omega,\bar{y},p)=\frac{2i}{\omega}\left(p_1\frac{D_{15}}{D}e^{m_1\bar{y}}-p_2\frac{D_{16}}{D}e^{m_2\bar{y}}+p_3\frac{D_{17}}{D}e^{m_3\bar{y}}-p_4\frac{D_{18}}{D}e^{m_4\bar{y}}\right) \tag{114}$$

$$K_{22}(\omega,\bar{y},p)=\frac{2}{\omega}\left(p_1\frac{D_{25}}{D}e^{m_1\bar{y}}-p_2\frac{D_{26}}{D}e^{m_2\bar{y}}+p_3\frac{D_{27}}{D}e^{m_3\bar{y}}-p_4\frac{D_{28}}{D}e^{m_4\bar{y}}\right) \tag{115}$$

Appendix B: Some useful integrals

To evaluate the third integral in closed form [Dag (2001)] in the right hand sides of Eqs. (46), (72) and (73), we would compute following integrals

$$C_n(A,t)=\int_A^\infty \frac{1}{\omega^n}\cos(\omega\cdot t)d\omega,\quad n=1,2,\cdots,N \tag{116}$$

$$S_n(A,t)=\int_A^\infty \frac{1}{\omega^n}\sin(\omega\cdot t)d\omega,\quad n=1,2,\cdots,N \tag{117}$$

For the case $n=1$, following results can be obtained

$$C_1(A,t)=-Ci(A\,|t|),\quad n=1,2,\cdots,N \tag{118}$$

$$S_1(A,t)=sign(t)(\frac{\pi}{2}-Si(A\,|t|)),\quad n=1,2,\cdots,N \tag{119}$$

where $Ci(\cdot)$ and $Si(\cdot)$ are defined as

$$Ci(t)=\gamma_0+In(t)+\int_0^t\frac{\cos\alpha-1}{\alpha}d\alpha \tag{120}$$

$$Si(t)=\int_0^t\frac{\sin\alpha}{\alpha}d\alpha,\quad n=1,2,\cdots,N \tag{121}$$

For the case $n>1$, integrals (114) and (115) can be evaluated by following recursive relations

$$C_n(A,t)=-\frac{1}{1-n}\frac{\cos(A\cdot t)}{A^{n-1}}+\frac{t}{1-n}S_{n-1}(A,t),\quad n>1 \tag{122}$$

$$S_n(A,t)=-\frac{1}{1-n}\frac{\sin(A\cdot t)}{A^{n-1}}-\frac{t}{1-n}C_{n-1}(A,t),\quad n>1 \tag{123}$$

Following formulae also used in the integration of asymptotic expressions

$$\int_0^\infty\frac{\sin(\omega\cdot\alpha)}{\omega}d\omega=\frac{\pi}{2}sign(\alpha),\quad n=1,2,\cdots,N \tag{124}$$